

# Scanning Tunneling Microscopy Studies of the Surfaces of a-Si:H and a-SiGe:H Films

Annual Subcontract Report  
1 December 1989 - 31 January 1991

A. Gallagher  
R. Ostrom  
D. Tannenbaum  
*National Institute of Standards and  
Technology  
Boulder, Colorado*

SERI technical monitor: W. Luft



Solar Energy Research Institute  
1617 Cole Boulevard  
Golden, Colorado 80401-3393  
A Division of Midwest Research Institute  
Operated for the U.S. Department of Energy  
under Contract No. DE-AC02-83CH10093

Prepared under Subcontract No. DB-4-04078-1

June 1991

**MASTER**  
DISTRIBUTION OF THIS DOCUMENT IS UNLIMITED

This publication was reproduced from the best available camera-ready copy submitted by the subcontractor and received no editorial review at SERI.

#### NOTICE

This report was prepared as an account of work sponsored by an agency of the United States government. Neither the United States government nor any agency thereof, nor any of their employees, makes any warranty, express or implied, or assumes any legal liability or responsibility for the accuracy, completeness, or usefulness of any information, apparatus, product, or process disclosed, or represents that its use would not infringe privately owned rights. Reference herein to any specific commercial product, process, or service by trade name, trademark, manufacturer, or otherwise does not necessarily constitute or imply its endorsement, recommendation, or favoring by the United States government or any agency thereof. The views and opinions of authors expressed herein do not necessarily state or reflect those of the United States government or any agency thereof.

Printed in the United States of America  
Available from:  
National Technical Information Service  
U.S. Department of Commerce  
5285 Port Royal Road  
Springfield, VA 22161

Price: Microfiche A01  
Printed Copy A03

Codes are used for pricing all publications. The code is determined by the number of pages in the publication. Information pertaining to the pricing codes can be found in the current issue of the following publications which are generally available in most libraries: *Energy Research Abstracts (ERA)*; *Government Reports Announcements and Index (GRA and I)*; *Scientific and Technical Abstract Reports (STAR)*; and publication NTIS-PR-360 available from NTIS at the above address.

## PREFACE

This is a final report on research carried out from December 1, 1989 to January 31, 1991 under Subcontract No. DB-4-04078-1 to the National Institute of Standards and Technology (formerly National Bureau of Standards). The principal investigator is Alan Gallagher, and additional contributors are Robert Ostrom and David Tannenbaum.

## ABSTRACT

The report contains a detailed description of the experimental complexities encountered in developing scanning tunneling microscope (STM) probing of atomic structure on the surface of freshly-grown hydrogenated-amorphous semiconductors. It also contains a speculative microscopic film-growth model that explains differences between the disorder in CVD grown a-Ge:H versus a-Si:H films. This model is derived from prior results obtained in the chemical analysis of GeH<sub>4</sub> plasmas, combined with surface reaction and thermodynamic considerations. The neutral radical fragments of silane, disilane and germane dissociation in discharges, which dominate the vapor and film-growth reactions, have been deduced from detailed analysis of prior data and are reported.

## SUMMARY

### OBJECTIVES

The primary objective of this research is to improve understanding of the microscopic physical and chemical phenomena responsible for hydrogenated amorphous silicon (a-Si:H) and silicon-germanium (a-Si:Ge:H) film growth, and for the resulting properties of the films. In previous years this primary emphasis was on mass spectroscopy of discharge gases, in order to achieve an understanding of the plasma gas and surface reactions. This year we have shifted our emphasis to diagnosing the structure and morphology of the growing film surface with atomic resolution.

### DISCUSSION

Our previous studies, combined with those at other laboratories, have led to a fairly complete understanding of the primary plasma and gas phase reactions that leads to a-Si:H and a-Si:Ge:H film growth in silane and silane-germane discharges. Analysis this year of our previous stoichiometry data on stable-gas and film production has led to an understanding of the initial silane and germane fragmentations, and thus has filled in one of the last major pieces of this picture. However, this understanding of the dominant microscopic pathways to film growth is not sufficient in itself to explain many causes of film-property changes. A more complete understanding of the growing film surface is needed. Models for the film growth reactions on the surface have also resulted from the above studies, and several conjectures have been offered regarding possible causes of semiconductor-quality variations in the resulting films. These conjectures are unsubstantiated, however, as no direct measurements of the atomic-scale features of the growing film surface have been made. Since only occasional film imperfections of atomic scale can have a major effect on photovoltaic properties, we believe it is now essential to measure the atomic-scale character of the growing surface that forms the a-Si:H thin film. We have therefore recently constructed a film surface diagnostic experiment, and we have devoted this contract year to developing procedures and interpretive methodology for film surface observations in this apparatus. The key surface diagnostic is a scanning tunneling microscope, which is housed in a UHV chamber attached to a film-deposition chamber. A low-energy-electron-diffraction apparatus and several surface preparation components are also used, as described in more detail below.

The second component of this year's research, already alluded to above, has been the interpretation and publication of discharge stoichiometry data from the previous year. Here we have diagnosed the measured stable-product yields in silane, germane, disilane and silane-germane discharges, where the stable products are film and stable gases such as higher silanes. This diagnosis has determined the initial fragmentations of  $\text{SiH}_4$ ,  $\text{GeH}_4$  and  $\text{Si}_2\text{H}_6$  into neutral radicals, due to electron collisions in these discharges. This is the initial step in the plasma chemistry that leads to film growth, and these fragmentations followed by radical reactions lead to the mixture of depositing species that largely determine film properties.

## CONCLUSIONS

Scanning-tunneling-microscope measurements of substrate surfaces, before a-Si:H deposition, have indicated that most polished crystal surfaces, with or without chemical cleaning and etching, are rough and irregular on an atomic scale. This suggests that some interface problems may be connected to resulting initial-growth inhomogeneities, and interface properties may depend strongly on surface preparations.

Analysis of our previous discharge stoichiometry data has yielded information on initial neutral-radical fragmentations that are the source of the radicals responsible for most film growth in these deposition discharges. Specifically, the primary fragmentation of  $\text{SiH}_4$  is to  $\text{SiH}_2 + 2\text{H}$ , of  $\text{GeH}_4$  is to  $\text{GeH}_3 + \text{H}$ , and of  $\text{Si}_2\text{H}_6$  is to  $\text{SiH}_3 + \text{SiH}_2 + \text{H}$ . These even-H radicals react with the parent gas to form higher silanes and germanes, the H reacts to form  $\text{SiH}_3$ ,  $\text{GeH}_3$  and  $\text{SiH}_4 + \text{SiH}_3$  respectively, and the  $\text{SiH}_3$  and  $\text{GeH}_3$  cause film growth. This analysis has also indirectly led us to a possible chemical explanation of the generally poorer semiconducting properties of a-Ge:H compared to a-Si:H. In essence, the  $\text{H}_2$ -elimination accompanied by Ge-Ge bonding that occurs subsequent to initial  $\text{GeH}_3$  attachment to the film is much more exothermic than for the equivalent Si film-growth process. This allows more distorted Ge-Ge bonds in the final film, compared to those in Si-based films.

## TABLE OF CONTENTS

Preface	2
Abstract	3
Summary	4
Table of Contents	6
1.0 Introduction	7
2.0 Amorphous Si and Ge Surface-Measurement Experiment	8
3.0 Analysis of Stable-product Stoichiometry in $\text{GeH}_4$ , $\text{Si}_2\text{H}_6$ , and $\text{SiH}_4/\text{GeH}_4$ Discharges	18
4.0 Proposed Cause of Poor a-Ge:H and a-Si:Ge:H Film Properties, and Suggested Methods of Improvement	19
5.0 References	22
6.0 Appendix: Title pages and abstracts of papers published, submitted for publication or prepared during the contract.	23

## SECTION 1.0

### INTRODUCTION

The objective of the experimental work during the contract year is to obtain scanning-tunneling microscope (STM) images of the morphology and chemical structure of as-grown a-Si:H and a-Si:Ge:H films, with atomic scale resolution. In order to discern surface shape due only to the film-growth process, we wish to start with substrates having clean crystal surfaces that are atomically flat over approximately  $1 \mu\text{m}$  square regions. Furthermore, after identifying such regions we must transfer the substrate into the deposition chamber, deposit a-Si:H film, return the substrate to the STM, and refind the originally-flat surface regions. We have constructed an apparatus for this purpose, and during the present contract we have also worked on the substrate preparation and analysis procedures and methods. We have found the substrate and probe-tip preparation procedures in particular to be very exacting and not very well documented in the STM and surface-science literature. As a consequence we have now developed considerable ancillary apparatus and in-vacuum preparation procedures. The apparatus procedures and results are described in the next section.

The second major activity during this contract period has been a very exacting diagnosis of data from previous contract periods regarding pure and mixed silane, germane, and disilane discharges. This has led to many results and conclusions that had not been originally apparent. Four manuscripts have now been prepared on these results, with three published or in process. (Two more manuscripts, concerning silane-disilane mixtures and silicon dust formation, still need to be organized and written.) This diagnosis has discerned the initial neutral fragmentation patterns of  $\text{SiH}_4$ ,  $\text{GeH}_4$  and  $\text{Si}_2\text{H}_6$  in these discharges, from the stable-product stoichiometries. This fragmentation, followed by radical-gas reactions, leads to the radical mixture which induces film growth and film properties.



## SECTION 2.0

### AMORPHOUS Si AND Ge SURFACE-MEASUREMENT EXPERIMENT

The basic method of this experiment is to discharge deposit a-Si:H, a-Ge:H and a-Si:Ge:H films, and then to measure the morphology and chemical character of the film surface with atomic resolution using a scanning tunneling microscope (STM). When this is done as a function of deposition conditions, it is expected that the quality and character of the bulk films will be discerned in the atomic-scale character of the growing surface.

The apparatus we have constructed to carry out these measurements is shown schematically in Fig. 1. Here film deposition is done in the turbomolecular-pumped chamber on the right side of the figure. After film deposition the deposition gas is evacuated and the substrate holder, which is mounted to a bellows, is translated to the center of the cross. There the transfer rod unscrews the substrate from the "Substrate Holder," transfers it into the ultrahigh vacuum (UHV) chamber on the left side of the figure, and screws it into the "Sample Holder." The manipulator then places the Sample Holder in the STM for analysis. The entire system is made of bakeable, Cu-sealed stainless steel high-vacuum components, and the discharge region can be heated to  $T_s$  between 20 and 450°C. When this is done the sample is cooled to ~20°C before diagnosis, first on the Transfer Rod Holder and then on the Sample Holder, as the STM requires stable temperatures.

The UHV chamber is initially pumped down with the turbomolecular pump, and is then baked at 150°C and pumped with an ion pump and Ti sublimation pump to  $\leq 10^{-10}$  Torr operating pressure. The deposition chamber is also oil-free and can be baked to achieve  $\sim 10^{-9}$  Torr vacuum, but it is more normally operated at  $\sim 10^{-8}$  Torr as it is frequently opened to transfer samples, substrates and STM tips in and out of the vacuum.

The character of the substrate surface prior to deposition is a very crucial aspect of the experiment. This issue has consumed the major part of our efforts throughout the present contract. For the purpose of diagnosing the initial substrate surfaces the UHV chamber also contains a low-energy electron-diffraction (LEED) apparatus. This diagnostic is sensitive to the cleanliness and crystal structure of the top layer of the substrate surface. It can also be operated in an Auger mode to measure impurities or chemical constituents on the surface. The LEED data represent an average over a  $\sim 1$  mm spot on the substrate, whereas the STM typically scans only  $\sim 1$   $\mu$ m wide regions. Thus, the LEED data are sensitive to surface inhomogeneities and overall structure, providing a valuable complement to the single-region STM data. The Ar<sup>+</sup> bombardment gun shown in Fig. 1 is used to sputter clean substrate surfaces by 1-2 eV Ar<sup>+</sup> bombardment. These substrates, most frequently Si crystals, are subsequently annealed by resistive or back-surface electron-bombarded heating, while held on the manipulator. (Electrical leads, etc. are not shown in Fig. 1.) The "Sample Cooling Arm" shown in Fig. 1 provides indirect water cooling of the sample holder during or after

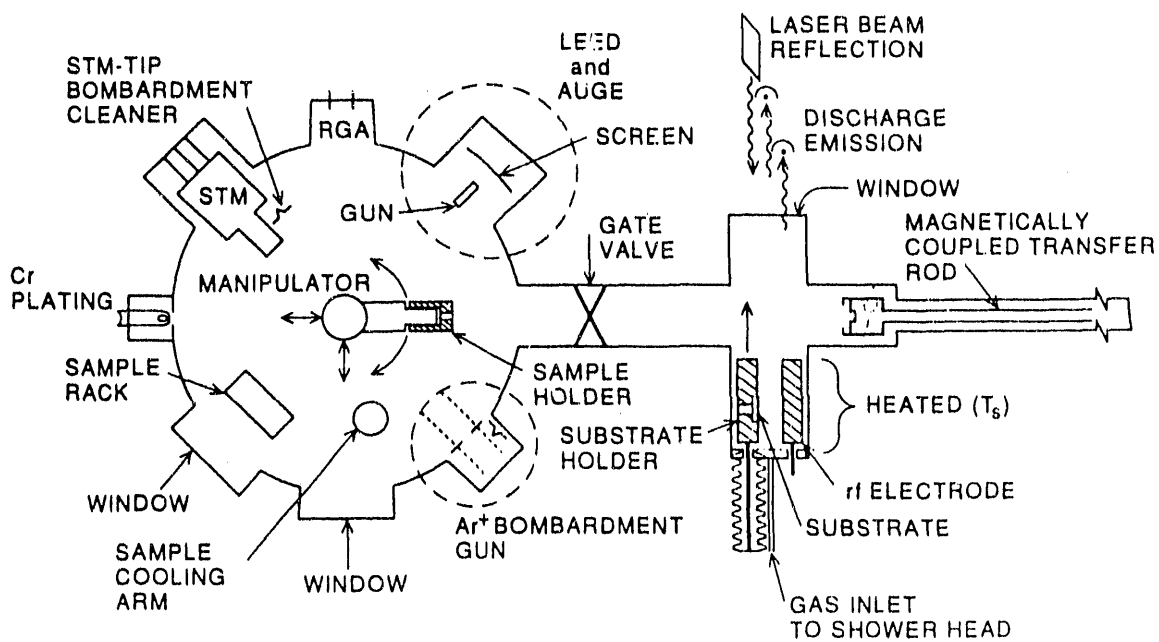


Fig. 1 Schematic of the film-deposition and diagnosis apparatus. The left, UHV chamber is ion and Ti-sublimation pumped while the right, film-deposition chamber is turbo-molecular pumped. The substrate holder is moved after deposition as indicated by the arrow, so that the transfer rod can remove and transfer the substrate to the UHV manipulator.

these annealing procedures. A chromium evaporator labeled "Cr Plating" is used for metalizing components and portions of substrates, as needed. A residual-gas-analyzer, labeled RGA, is used to analyze discharge and residual vacuum gases. The tip bombardment heater is used to electron-beam heat STM tips, particularly tungsten tips, to clean their surface.

The STM is the most important part of the apparatus, and is shown in more detail in Fig. 2. This is a two-tube STM, originally constructed and sold by McAllister Services, based on a design by Lyding.<sup>1</sup> We have greatly modified many features of the original instrument in order to achieve acceptable operation, but the design principle is still that shown in Fig. 2. There the metal-plating on the inner piezoelectric tube is divided into quadrants, and opposing voltages are applied to opposite quadrants to bend the tube. This produces the "x" and "y" motions of the raster scans, while equal voltage increments to all quadrants provides "z" motion toward or away from the sample. The "sample," which is also the discharge substrate in our experiment, is attached to the end of a hollow cylinder "Sample Holder," as shown in Fig. 2. This cylinder slides on two parallel rods that are supported by a partially cut away quartz tube, which is in turn attached to the outer piezoelectric cylinder. The manipulator places the sample holder on these rods with several millimeter gap between tip and sample, and the sample is then moved along the rods into tunneling range at about 5Å tip-sample separations. This tip-approach is accomplished by repetitively applying a sawtooth voltage (z displacement) to the outer piezoelectric tube, causing repeated inertial slippage of the sample holder along the rods.

Surface analysis is most frequently done by raster scanning a 100 to 10,000Å square region at constant tunneling current ( $i$ ) and gap voltage ( $V$ ), thereby achieving a topological map of the surface. Examples of the observed topologies are given in Figs. 3-6; these will be discussed below. A second type of "spectroscopic" data, commonly used on semiconductors, is obtained from a measurement of  $i$  versus  $V$  at constant  $x$ ,  $y$ , and  $z$ , generally for  $-3 \leq V \leq 3$  volts. This measurement is sensitive to the surface local electron or hole state density, and is used to observe different atomic species on the surface as well as surface bond reconstructions. A third data mode is  $i$  versus gap length ( $z$ ) at a point, which is sensitive to the tunneling barrier height and thus also to surface species on tip and substrate. For clean sample and tip surfaces  $i \propto \exp(-Z/L)$  where  $L \cong 1-2\text{\AA}$ , characteristic of electron tunneling through a vacuum work-function barrier of several eV and a  $\sim 5\text{\AA}$  gap. The tip height  $z$  versus  $x$  and  $y$  can also be considered a map of constant substrate electron density above the surface, in the absence of the probe.

The atomic wave-function variations at a surface typically induce 0.1-1Å height variations in STM-measured surface topology. In order to observe these the tip-substrate gap  $z$  must be stable to comparable or smaller distances. The tip and sample supporting structure has dimensions of cm, so  $\Delta l/l < 10^{-9}$  is necessary. This requires exceptional vibration isolation, rigid structures, and low thermal drift. Moderate thermal drifts (1°C/hr) are tolerable, as raster scans typically require 1-10 minutes and the linear portion of the drift can be removed during computer image reconstruction. However, heating of samples and tips to

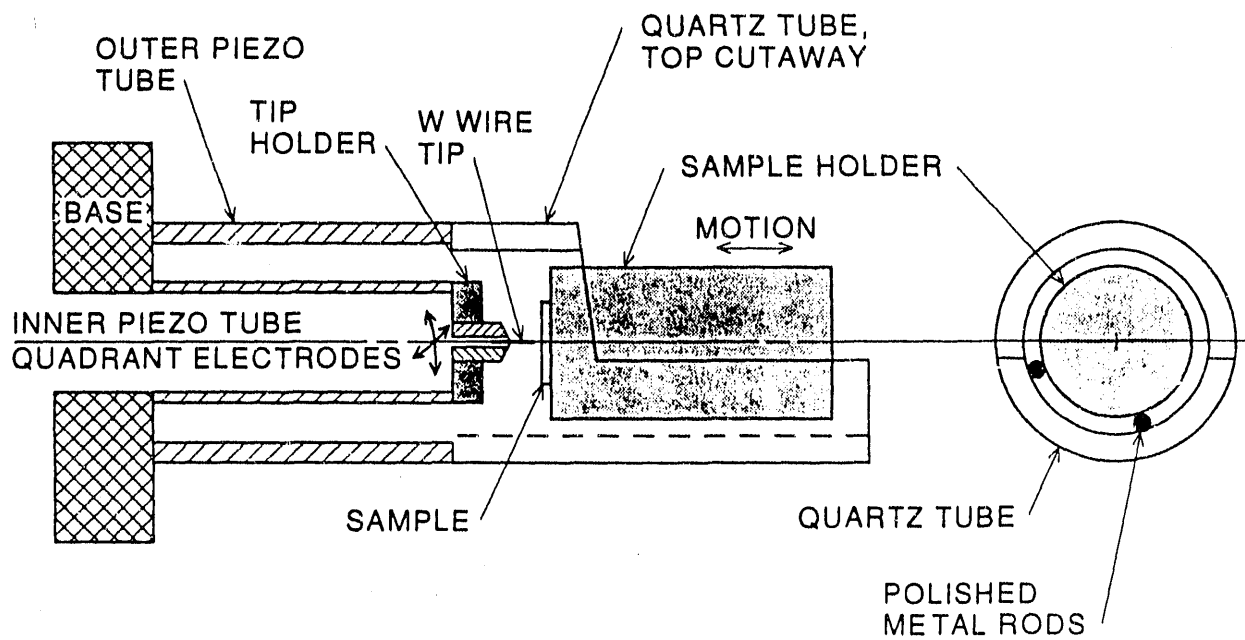


Fig. 2 Cross section and end view of the Lyding two-tube STM design, as adapted by McAllister in the STM we are using. The piezo tubes are  $\sim 0.5''$  and  $0.75''$  diameter.

hundreds or even  $> 1000^{\circ}\text{C}$  is often a required preparation for film deposition, and these must be thoroughly recooled before inserting into the STM. We use a small W-filament lamp inside our UHV chamber to minimize the net STM thermal drift during moderate residual sample cooling. By adjusting the power to this lamp, typically a few watts, the  $< < 1\%$  that is absorbed by the STM balances the slow cooling effect and allows scans without running out of range.

The other critical factor dictated by  $\Delta l/l < 10^{-9}$  is STM structural rigidity and very thorough vibration isolation. Laboratories generally have very large vibrations in the 1-120 Hz region, partly due to building motions and resonances, and these can produce very severe STM-gap fluctuations. It is common practice to place STM's in the quietest possible locations on solid ground far from pumps, etc., but we did not have that option available. Even in quiet sites most vacuum STM's are hung from two sets of three springs working in series, often with a copper ring at the junction and magnets attached to the chamber nearby to provide eddy-current damping of the first stage. Our commercial instrument had totally inadequate structural rigidity and vibration isolation, and we have completely reconstructed both the device and its suspension from the vacuum chamber. Another major source of tip-current and z noise can result from magnetic fields in laboratories, typically from power lines, pumps, computer cables and monitors. To reduce this problem to an acceptable level we have installed our tip-current amplifier chip directly on the STM inside the vacuum chamber.

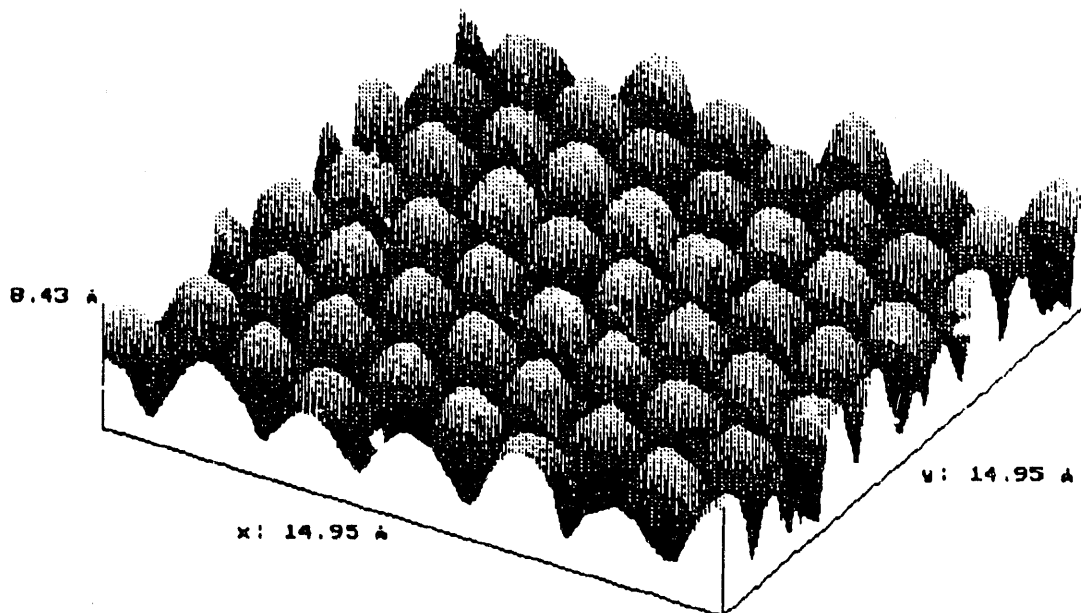
An important factor in STM surface analysis is to avoid damaging or modifying the surfaces under study. This damage can have two types of causes. One is direct tip-substrate contact, which can gouge substrates, transfer atoms along and between tip and substrate, and deposit debris about both. The second type of damage results from excessive tunneling voltage or current. This can also transfer material, blast holes or pile up material on substrates; effects that are readily seen in subsequent tunneling-current noise or surface scans. However, much smaller, more subtle effects, such as induced surface reconstruction or atomic diffusion can also occur. Most of these have been identified on crystal surfaces; we expect them to be more severe on a-Si:H and a-Si:Ge:H surfaces. We have discerned many of these effects during our work under this contract, and we are continually improving our apparatus and procedures to minimize and eventually eliminate them. One example of an important procedure, already mentioned above, is probe-tip cleaning by electron-bombardment heating in UHV. This removes oxide layers and debris, either of which can cause erratic tunneling, atom-motion and misleading spectroscopic and topology results.

A primary objective of our measurements is to detect the shapes, sizes and chemical character of incipient voids in growing a-Si:H and related films. We expect to see these as valleys and pits in the growing surface, and perhaps as H-rich regions. From x-ray diffraction, NMR, film density and other known bulk-film characteristics we expect these voids to be present and to play an important role in film properties.<sup>2</sup> In order to unambiguously detect these surface irregularities in the growing film surface we wish to deposit the film on an atomically flat and defect-free region of a substrate. This region should preferably be of the order of  $1 \mu\text{m}$  square or larger, and we should be able to find it repeatedly after growing successive film

layers on it. Furthermore, we need several substrate materials, one of which should be Si, to ensure that we are observing universal characteristics of a-Si:H.

A major part of the research effort during the contract has been devoted to achieving this unusually stringent substrate-preparation and placement goal. We have so far achieved  $> 1 \mu\text{m}$ , atomically-flat regions only on pyrolytic graphite and on GaAs crystals, and even these generally have atomic imperfections at 30-300Å typical spacings. We have studied a variety of traditional crystal-Si surface-preparation techniques, but so far have been unable to obtain large ( $\sim 1 \mu\text{m}$ ) atomically-flat regions with relatively few irregularities. (We do obtain excellent LEED patterns of reconstructed surfaces, as expected, but these apparently result from many small flat regions and are insensitive to an occasional irregularity therein.) In the case of pyrolytic graphite the surface is "prepared" by simply peeling off top layers with tape. This surface, whose atomic features are shown in Fig. 3, is useful but very easily damaged during STM probing and discharge deposition, and is not ideal for the present experiment. The flat GaAs surface is prepared by cleaving along a crystal plane in vacuum. When done well this produces large ( $> 100 \mu\text{m}$ ) atomically flat regions with only occasional debris and atomic irregularities. This surface is much more easily STM-damaged than is crystal Si, but this is so far our best substrate surface. A GaAs topology example is shown in Fig. 4. The y-direction curvature seen there is a thermal drift artifact; the surface is atomically flat except for a few attached atoms or molecules seen as hills. A higher resolution scan of a GaAs surface several hours after cleaving, in Fig. 5, shows a partial monolayer of absorbed atoms. Si cannot be easily cleaved, and we have concentrated on traditional chemical and annealing methods of preparing (100) and (111) crystal surfaces. An example of crystal Si surface irregularities we typically obtain is shown in Fig. 6. This surface is not deemed to be sufficiently flat and fault-free to be used in our study a-Si:H deposition. It is particularly deficient for studying microparticulate deposition from discharges, as it already has some equivalent features. These Si surfaces, and others that show similar surface irregularities, were prepared from highest-quality polished Si wafers by standard wafer-preparation techniques. These techniques include various chemical oxidations, etchings and passivations before introduction into the vacuum chamber as well as ion-bombardment cleaning and a variety of thermal annealing procedures in UHV. We are continuing to investigate new preparation procedures, to achieve the desired large, low-defect Si surface regions.

At the start of this contract we had the commercial STM in operation in the above-described vacuum system. However, the STM proved to be totally inadequate for obtaining atomic-resolution images in vacuum. We therefore spent a major portion of the present contract redesigning and improving the instrument and tip-preparation methods, and as a result we now have achieved the desired atomic resolution. Our second major need is for "large-area," atomically flat and defect free substrate surfaces, and the other major portion of the present contract has been devoted to this problem. Considerable progress has been made, as described above, but this is still not fully achieved for Si substrates. Thus we have so far done minimal diagnosis of a-Si:H deposits, and we do not have any significant results regarding their atomic-level morphology and chemical character.



File	18-g11
Setpoint	2 nA
Bias	9.768 mV

Fig. 3 Our STM image of atoms on a pyrolytic graphite surface, taken in vacuum with 10 mV sample bias and 2 nA tip current.

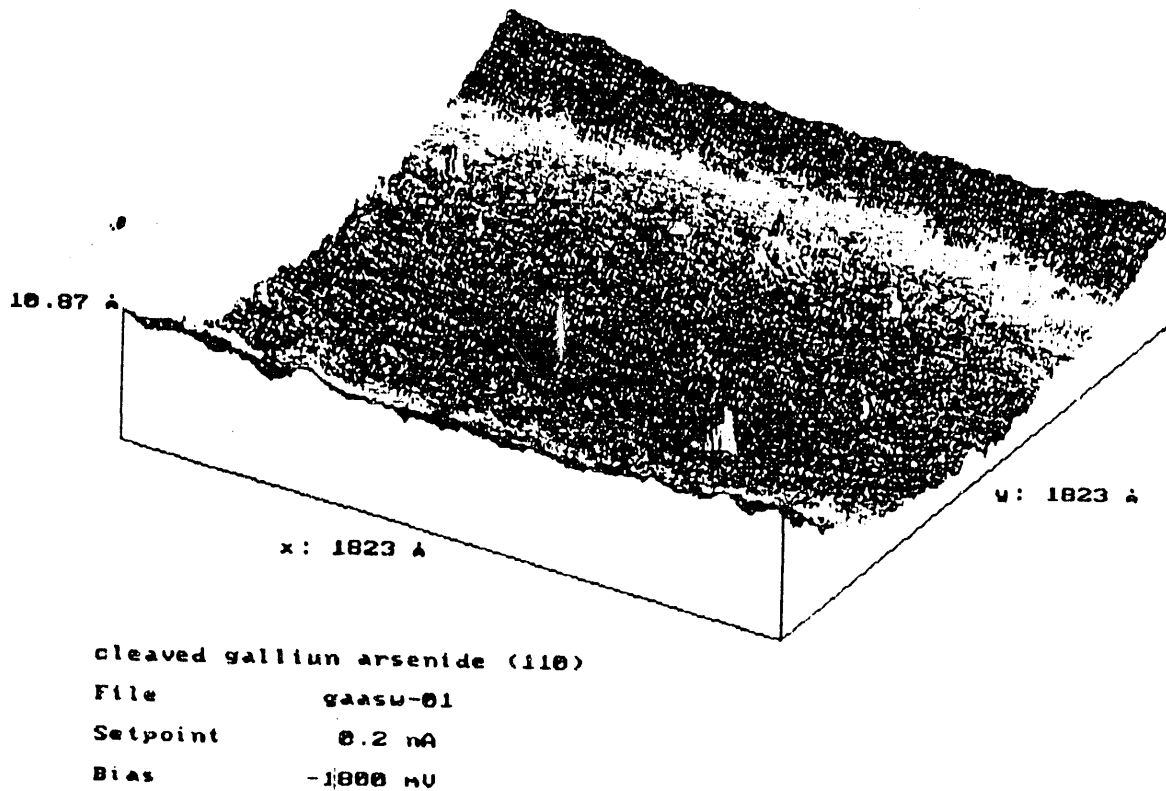
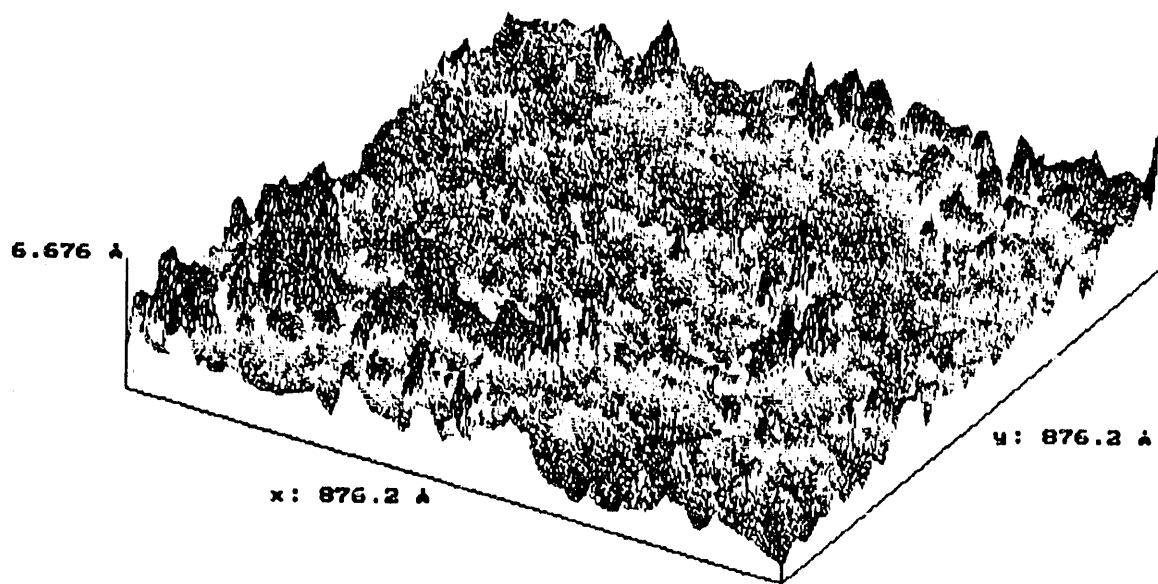


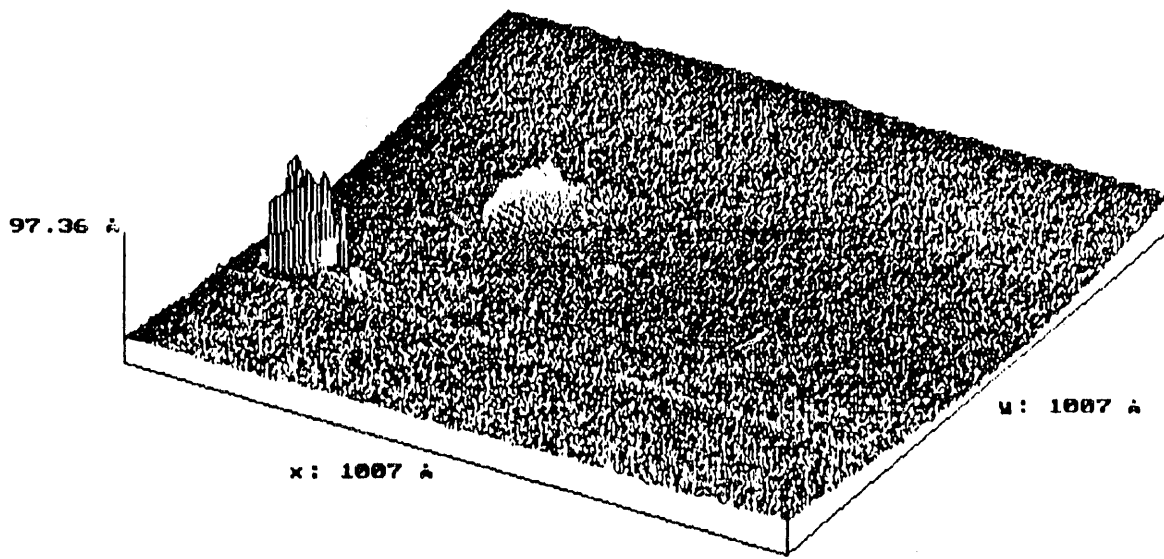
Fig. 4 STM image of a 1823Å square region of a GaAs crystal cleaved in vacuum.





cleaved gallium arsenide (110)  
File            gaasu-17  
Setpoint        0.2 nA  
Bias            -1800 mV

Fig. 5 STM image of a GaAs (110) surface several hours after cleaving, showing a partial monolayer of adsorbed atoms.



si (100) p-type pt tip positive bias  
File si-03  
Setpoint 1 nA  
Bias 1500 mV

Fig. 6 STM image of a Si (100) surface loaded after etching and oxidizing, then thermally cleaned of oxide in vacuum.

## SECTION 3.0

### ANALYSIS OF STABLE-PRODUCT STOICHIOMETRY IN $\text{GeH}_4$ , $\text{Si}_2\text{H}_6$ , AND $\text{SiH}_4/\text{GeH}_4$ DISCHARGES

We have measured, during previous contract periods, the stable-gas and film growth stoichiometry in discharges of  $\text{SiH}_4$ ,  $\text{GeH}_4$ ,  $\text{Si}_2\text{H}_6$  and mixtures of these gases. (Here "stoichiometry" refers to quantitative analysis of all stable products as fractions of the decomposed feed gases, so that all Si, Ge, and H atoms are accounted for in the products.) We had also diagnosed the  $\text{SiH}_4$  data and submitted the results for publication. This analysis and its results explain the sequence of events that lead to a-Si:H films. Specifically, we discerned what mixture of neutral radicals were produced in the  $\text{SiH}_4$  dissociations (primarily  $\text{SiH}_2 + 2\text{H}$ ), and how these reacted in the vapor and on the growing film surface.

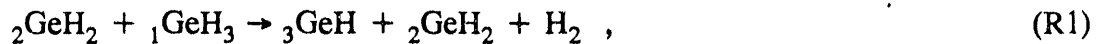
During the present contract we have completed a detailed diagnosis of our stoichiometry data for pure  $\text{GeH}_4$  and  $\text{Si}_2\text{H}_6$ , as well as in  $\text{GeH}_4/\text{SiH}_4$  mixtures. The results have been extremely interesting and much more definitive than we had initially thought was possible, particularly for the very complicated chemical system of  $\text{GeH}_4/\text{SiH}_4$  mixtures. The results of these analyses have been prepared or submitted for publication, and the cover pages and abstracts are included in the Appendix. Highlights of these results are summarized in those abstracts. These analyses led to the conclusion that film growth mechanisms in  $\text{Si}_2\text{H}_6$  discharges are very similar to those in  $\text{SiH}_4$  discharges, and there is negligible basis for substituting disilane for silane in a-Si:H film production. The  $\text{GeH}_4$  discharge analysis led us to recognize that the plasma-produced radicals responsible for a-Ge:H film growth were mostly  $\text{GeH}_3$ , in exact analogy to the  $\text{SiH}_3$  primarily responsible for a-Si:H film growth. Thus, we were driven to look for other causes of the much poorer semiconductor quality of a-Ge:H films. We have now identified a feasible basis for this well-known problem, based on film-growth reaction chemistry. This is explained in the next section.

## SECTION 4.0

### PROPOSED CAUSE OF POOR a-Ge:H AND a-Si:Ge:H FILM PROPERTIES, AND PROPOSED METHODS OF IMPROVEMENT

Inferior semiconductor properties are almost universally obtained for amorphous germane (a-Ge:H) films. In contrast, a-Si:H films deposited by many techniques attain excellent photovoltaic properties. As described in the following paragraph, we believe this may be due to chemical constraints in the film growth step where Ge-H bonds in the surface layers change to Ge-Ge bonds of the final, mostly Ge film.

The initial bonding of  $\text{GeH}_3$ , or occasionally other H-rich germane radicals, to the a-Ge:H film surface by a Ge-Ge bond produces a very H-rich surface layer. In contrast, the bulk  $250^\circ\text{C}$  film contains only 5-10 atomic percent H. The conversion of these  $\text{GeH}_3$ ,  $\text{GeH}_2$ , and similar groups attached to the surface to the primarily Ge-Ge bonded film is believed to occur predominately by a sequence of exothermic  $\text{H}_2$  elimination reactions. In each of these reactions two Ge-H bonds convert to a Ge-Ge bond and an H-H bond with release of an  $\text{H}_2$  molecule. An example is



where the subscript before each Ge refers to its number of Ge-Ge bonds to other Ge in the film. This reaction is shown diagrammatically in Fig. 7a. The enthalpy change of (R1) is

$$\Delta H_1 = 2 \Delta H(\text{Ge-H}) - \Delta H(\text{Ge-Ge}) - \Delta H(\text{H}_2), \quad (1)$$

where  $\Delta H(\text{A-B})$  refers to the (positive) AB bond dissociation energy. The  ${}_n\text{Ge-H}$  and  ${}_n\text{Ge-}{}_m\text{Ge}$  bond energies are expected to vary with  $n$  and  $m$ , since they depend on adjustments in the remaining bonds when the H is released or Ge is attached. Thus, in general  $\Delta H_1$  will depend on  $n$  and  $m$ . We will assume, however, that we can define average Ge-H and Ge-Ge bond dissociation energies such that the various reactions (R1) can be characterized by a single quantity  $\Delta H_1$ . Now we note that such reactions are precisely those that are implied by the heat of formation reactions of  $\text{GeH}_4$ . This allows us to quantify  $\Delta H_1$  in terms of this well-known thermodynamic quantity. The  $\text{GeH}_4$  heat of formation  $\Delta H_f^\circ(\text{GeH}_4)$  is the total energy change from the standard states of  $\text{H}_2$  plus solid, crystalline Ge; i.e.



This corresponds to breaking two crystalline Ge-Ge bonds per vaporized Ge, breaking two H-H bonds, and forming the four Ge-H bonds of  $\text{GeH}_4$ . Comparing this to Eq. (1) and summing over successive Ge bonds one sees that

$$\Delta H_f^\circ(\text{GeH}_4) = -2(\Delta H_1). \quad (2)$$

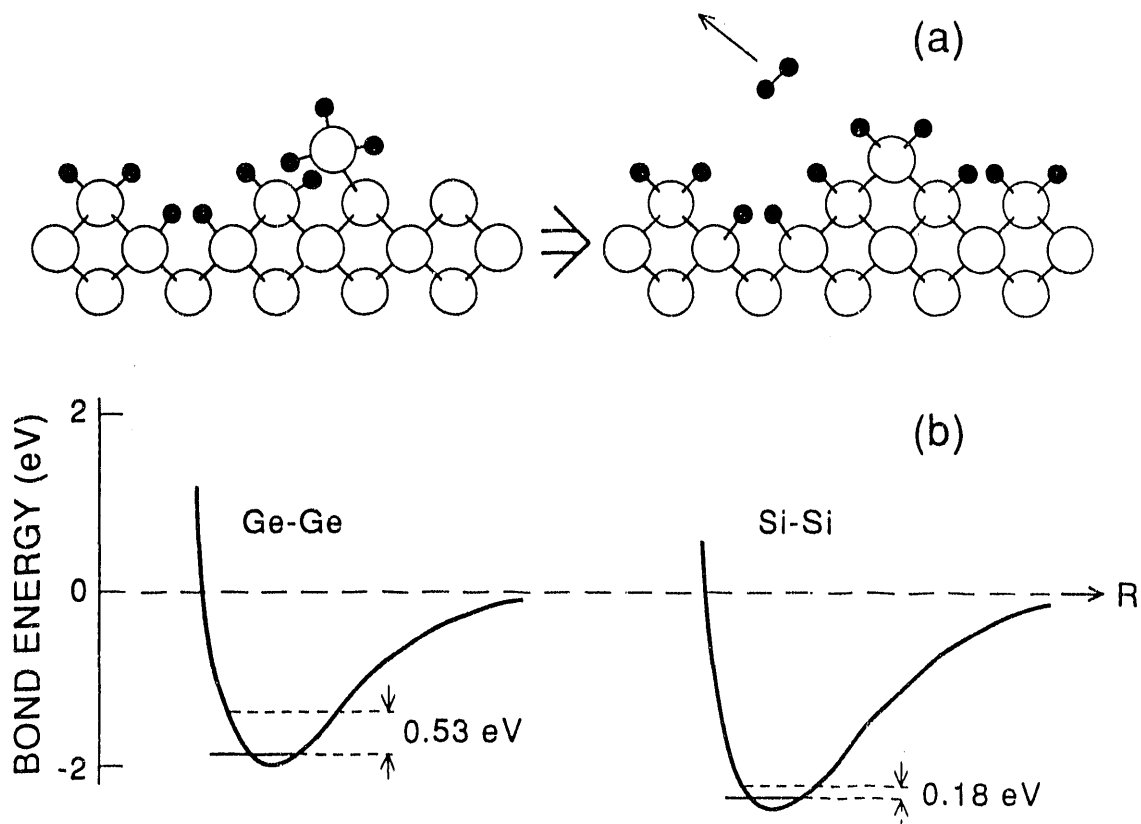


Fig. 7 (a) Diagrammatic example of the H<sub>2</sub> elimination surface reactions that transfer the H-rich surface to the H-poor bulk a-Ge:H and a-Si:H films. Small solid circles represent H atoms, and large open circles represent Si or Ge atoms. (b) Diagrammatic representation of the dependence of bond energy on internuclear separation R in a-Ge:H and a-Si:H films. The energy widths of 0.53 eV and 0.18 eV are the average excess energy available in the H<sub>2</sub>-elimination reactions.

In essence, the film-growth process of turning GeH bonds into crystalline Ge plus H<sub>2</sub> is the inverse of turning H<sub>2</sub> and solid Ge into GeH<sub>4</sub>, and the bond sums must be conserved.

The Ge-Ge bond strength is shown diagrammatically as a function of Ge-Ge spacing in Fig. 7b, where the crystalline bond energy is 1.92 eV. Since  $\Delta H_f^\circ(\text{GeH}_4) = 1.06 \text{ eV} = -2(\Delta H_1)$ , 0.53 eV average excess energy is available in R1 as shown in Fig. 7b. Thus, on average the Ge-Ge bond formed during R1 can be nearly 0.53 eV weaker than the crystal bond strength before reaction exothermicity and irreversibility is lost. Thus, as seen in Fig. 7b, the resulting Ge-Ge bond can be severely distorted compared to the crystalline value. Such distortions, in bond angle as well as length, become buried under successive growth layers and can ultimately lead to a poor semiconductor.

Reactions (R1) and (R2) and Eqs. (1) and (2) have silicon analogues, and comparing these Si and Ge cases is very enlightening.  $\Delta H_f^\circ(\text{SiH}_4) = 0.36 \text{ eV}$ , so the average H<sub>2</sub> elimination reaction (R1) is exothermic by 0.18 eV for Si compared to 0.53 eV for Ge. Thus, as shown in Fig. 7b, the Si-Si bond length must be much closer to the crystalline value of 2.32 eV. In essence the (R1) reaction exothermicity determines how far the Ge-Ge or Si-Si bonds can be from crystalline order before the H<sub>2</sub> elimination is inhibited by endothermicity, and we are suggesting that this largely determines the degree of disorder in the final film. Due to the much larger energy excess for Ge, the problem of forming well structured a-Ge:H is much more severe than for a-Si:H.

This model suggests that a-Ge:H and a-Si:Ge:H structure can be improved by introducing surface rearrangements or weak etching during deposition, leading to stronger final Ge-Ge bonding. Examples of such methods are introducing other chemical reactants, or a large rate of relatively low-energy surface bombardments. An example of the former is the use of fluorinated compounds, and of the latter is film growth on the powered electrode or adding Ar to the discharge. Both approaches are known to improve a-Ge:H film quality.<sup>3,4</sup>

## SECTION 5.0

### REFERENCES

1. J. W. Lyding, S. Skala, J. S. Hubacek, R. Brockenbrough, and G. Gammie, Rev. Sci. Instrum. 59, 1897 (1990).
2. A. H. Mahan, D. L. Williamson, B. P. Nelson, and R. S. Crandall, Phys. Rev. B, 40, 12024 (1989).
3. S. Guha, J. Yang, A. Pawlikiewicz, T. Glatfelter, R. Ross, and S. R. Ovshinsky, 1988 Proceedings of the 20th Photovoltaic Specialists Conference, Las Vegas, Nevada, p. 79.
4. K. D. Mackenzie, J. R. Eggert, D. J. Leopold, Y. M. Li, and W. Paul, Phys. Rev. B 31, 2198 (1985).

## SECTION 6.0

### APPENDIX

Title pages and abstracts of papers prepared under this contract

- D. A. Doughty and A. Gallagher, "Spatial distribution of a-Si:H film-producing radicals in silane rf glow discharges," J. Appl. Phys. 67, 139 (1990).
- D. A. Doughty and A. Gallagher, "Causes of SiH<sub>4</sub> dissociation in silane dc discharges," Phys. Rev. A 42, 6166 (1990).
- J. R. Doyle, D. A. Doughty and A. Gallagher, "Silane dissociation products in deposition discharges," J. Appl. Phys. 68, 4375 (1990).
- J. R. Doyle, D. A. Doughty and A. Gallagher, "Germane discharge chemistry," J. Appl. Phys., in press.
- J. R. Doyle, D. A. Doughty and A. Gallagher, "Plasma chemistry in disilane discharges," J. Appl. Phys., submitted.
- J. R. Doyle, D. A. Doughty and A. Gallagher, "Plasma chemistry in mixtures of silane, germane, and disilane," J. Appl. Phys., in preparation.

*abstracts removed.*  
*As*



<b>Document Control Page</b>	<b>1. SERI Report No.</b> SERI/TP-214-4409	<b>2. NTIS Accession No.</b> DE91002169	<b>3. Recipient's Accession No.</b>
<b>4. Title and Subtitle</b>  Scanning Tunneling Microscopy Studies of the Surfaces of a-Si:H and a-SiGe:H Films		<b>5. Publication Date</b> June 1991	
		<b>6.</b>	
<b>7. Author(s)</b>  A. Gallagher, R. Ostrom, D. Tannenbaum		<b>8. Performing Organization Rept. No.</b>	
<b>9. Performing Organization Name and Address</b>  National Institute of Standards and Technology Boulder, Colorado		<b>10. Project/Task/Work Unit No.</b> PV141101	
		<b>11. Contract (C) or Grant (G) No.</b>  (C) DB-4-04078-1  (G)	
<b>12. Sponsoring Organization Name and Address</b> Solar Energy Research Institute 1617 Cole Blvd. Golden, CO 80401-3393		<b>13. Type of Report &amp; Period Covered</b> Technical report, 1 December 1989 - 31 January 1991	
		<b>14.</b>	
<b>15. Supplementary Notes</b> SERI technical monitor: W. Luft, (303) 231-1452			
<b>16. Abstract (Limit: 200 words)</b>  This report describes the experimental complexities encountered in using scanning tunneling microscopy (STM) probing for the atomic structure of the surface of freshly grown, hydrogenated-amorphous semiconductors. The report also contains a speculative microscopic film-growth model that explains differences between the disorder in a-Si:H and a-SiGe:H films grown by chemical vapor deposition (CVD). The model is derived from prior results obtained in the chemical analysis of GeH <sub>4</sub> plasmas, combined with surface-reaction and thermodynamic considerations. The neutral radical fragments of silane, disilane, and germane dissociation in discharges, which dominate the vapor and film-growth reactions, were deduced from a detailed analysis of prior data; these fragments are also reported.			
<b>17. Document Analysis</b> a. Descriptors photovoltaics ; solar cells ; amorphous state ; silicon ; microscopes ; film growth  b. Identifiers/Open-Ended Terms  c. UC Categories 271			
<b>18. Availability Statement</b> National Technical Information Service U.S. Department of Commerce 5285 Port Royal Road Springfield, VA 22161		<b>19. No. of Pages</b>  29	
		<b>20. Price</b>  A03	

**END**

**DATE  
FILMED**

*08/09/91*